J Solid State Electrochem (2007) 11:915–921
DOI 10.1007/s10008-007-0311-7

ORIGINAL PAPER

Activation of methanol-tolerant carbon-supported $RuSe_x$ electrocatalytic nanoparticles towards more efficient oxygen reduction

Aneta Kolary-Zurowska · Agata Zieleniak · Krzysztof Miecznikowski · Beata Baranowska · Adam Lewera · Sebastian Fiechter · Peter Bogdanoff · Iris Dorbandt · Roberto Marassi · Pawel J. Kulesza

Received: 19 January 2007 / Revised: 14 March 2007 / Accepted: 16 March 2007 / Published online: 21 April 2007

Abstract An electrocatalytic system that utilizes tungsten oxide modified carbon-supported $RuSe_x$ nanoparticles is developed and characterized here using transmission electron microscopy and such electrochemical diagnostic techniques as cyclic voltammetry and rotating ring-disk voltammetry, as well as upon its introduction (as cathode) to the low-temperature hydrogen–oxygen fuel cell. After the modification of $RuSe_x$ catalytic centers with ultra-thin films of WO_3, the potential of oxygen reduction in 0.5 mol dm^{-3} H_2SO_4 (in the absence and presence of methanol) is shifted ca. 70 mV (under rotating disk voltammetric conditions) towards more positive values, and the percent formation (at ring) of the undesirable hydrogen peroxide has decreased approximately twice when compared to the WO_3-free system. Relative to bare electrocatalyst, an increase of power density from 75 to 100 mW cm^{-2} (at 300 mA cm^{-2}) has been observed upon utilization of WO_3-modified $RuSe_x$ in polymer electrolyte membrane fuel cell at 80 °C. In comparison to Vulcan-supported Pt nanoparticles, the overall electrocatalytic performance of tungsten oxide modified carbon-supported $RuSe_x$ nanoparticles is lower, but the latter system is practically insensitive to the presence of methanol even at 0.5 mol dm^{-3} level.

Keywords Oxygen reduction · Selenium modified ruthenium · Tungsten oxide overlayers · Acid electrolyte · Rotating ring-disk voltammetry · Hydrogen-oxygen fuel cell

Dedicated to Professor Dr. Algirdas Vaskelis on the occassion of his 70th birthday.

A. Kolary-Zurowska · A. Zieleniak · K. Miecznikowski · B. Baranowska · A. Lewera · P. J. Kulesza (✉)
Department of Chemistry, University of Warsaw,
Pasteura 1,
02-093 Warsaw, Poland
e-mail: pkulesza@chem.uw.edu.pl

S. Fiechter · P. Bogdanoff · I. Dorbandt
Hahn-Meitner-Institut, Abt. Solare Energetic,
Glienicker Str. 100,
14109 Berlin, Germany

R. Marassi
Department of Chemistry, University of Camerino,
S. Agostino 1,
62032 Camerino, Italy

Introduction

There has been a growing recent interest in the development of fuel cells as alternative electrochemical devices for efficient generation of energy [1–5]. Among the applicable low-temperature acid-type systems, polymer electrolyte membrane fuel cells (PEMFCs) and direct methanol fuel cells (DMFCs) are probably the most promising devices, and they are subjects of interest in many laboratories worldwide. While in the case of PEMFCs, hydrogen is utilized; the methanol fuel is oxidized in the anodic compartment of DMFCs. To improve power densities of both PEMFCs and DMFCs, there is a need to increase electrocatalytic activities of cathode materials to achieve the efficient four-electron reduction in oxygen to water:

$$O_2 + 4H^+ + 4e^- \leftrightarrow 2H_2O \quad (1)$$

The latter reaction proceeds at the theoretical standard potential of 1.23 V (versus RHE). Less efficient electroreduction of oxygen is a two-step process involving first two-electron reduction to the hydrogen peroxide intermediate,

$$O_2 + 2H^+ + 2e^- \rightarrow H_2O_2 \quad (2)$$

proceeding at the standard potential of 0.67 V then followed by further reduction to H_2O,

$$H_2O_2 + 2H^+ + 2e^- \rightarrow 2H_2O \quad (3)$$

at the standard potential of 1.76 V. In reality, all above processes are kinetically slow, and they occur with high overvoltages, i.e., at much more negative (than standard) potentials even upon application of noble metal (Pt or Pt-based alloy) electrocatalysts. Typically, diagnostic voltammetric measurements utilizing rotating ring-disk electrode (RRDE) assembly are performed to determine kinetic parameters and to comment on the relative formation (at ring) of hydrogen peroxide during the oxygen electroreduction (at disk) [6–10].

At present, four types of electrode materials are most commonly considered for the electrocatalytic reduction in oxygen in acid media. The highest electrocatalytic activities are achieved with the use of nanoparticles of platinum and its alloys with other metals [11–14]. Macrocyclic compounds, including porphiryn and phtalocyanine complexes of cobalt and iron [15–17], as well as certain metal oxides (spinels and perovskites) [18–20], are often considered as alternate electrocatalytic systems. Efforts have also been made to develop catalysts that are tolerant to methanol. They include cluster-like materials of the type of Ru_xSe_y, Ru_xS_y, or $Mo_xRu_ySe_z$ nanoparticle chalcogenides [21–26] that have been reported to exhibit catalytic activity even higher than Pt nanoparticles during the reduction in oxygen in the presence of methanol. Because of methanol crossover occurring through the solid electrolyte membrane from the anode to the cathode in DMFC, the simultaneous oxygen reduction reaction and oxidation of methanol at the cathode results in mixed potential and, consequently, in the reduction in the cell performance. Development of highly active, methanol-tolerant cathode catalysts is, therefore, of primary importance to the development of DMFCs.

After our preliminary communication [25], we pursue here the concept of modification of $RuSe_x$ nanoparticles with tungsten oxide to activate them towards efficient electroreduction of oxygen. To avoid a decrease in population of reactive centers and to minimize ohmic loses in the film, care has been exercised to produce ultra-thin (on the level of tens of nm) layers of WO_3 on carbon-supported $RuSe_x$ nanoparticles. It was previously reported [27] that tungsten oxide exhibited electrocatalytic properties towards reduction in H_2O_2. It is reasonable to expect that WO_3-modified $RuSe_x$ acts as a bifunctional system, in which oxygen reduction is primarily induced at $RuSe_x$ catalytic centers; whereas reduction in any hydrogen peroxide intermediate is further activated at the tungsten oxide matrix. In the present work, we also address electrocatalytic reactivity of WO_3-modified $RuSe_x$ nanoparticles in the presence of methanol. Further, comparison has been made to the behavior of Vulcan-supported Pt nanoparticles under the analogous RRDE voltammetric conditions. Finally, we test the performance of WO_3-modified $RuSe_x$ as cathode (together with conventional Pt anode) in the hydrogen–oxygen polymer electrolyte membrane fuel cell.

Experimental

All chemicals were commercial materials of the highest available purity and were used as received. Solutions were prepared from triply-distilled subsequently-deionized water. They were deaerated (using argon) or saturated with oxygen for at least 10 min before the electrochemical experiment. Experiments were conducted at room temperature (20±0.5 °C).

The electrochemical experiments were performed with CH Instruments (Austin, TX) Model 750A workstation. A mercury/mercury sulfate electrode (Hg/Hg_2SO_4), which potential was 640 mV more positive relative to the reversible hydrogen electrode (RHE), was used as a reference electrode. This electrode was placed in the second compartment and connected to the main cell through a lugging capillary. All potentials are expressed against the reversible hydrogen electrode (RHE).

Rotating disk electrode (RDE) and RRDE voltammetric measurements were accomplished using a variable speed rotator (Pine Instruments, USA). The electrode assembly utilized a glassy carbon disk and a Pt ring. The electrodes were polished with successively finer grade aqueous alumina slurries (grain size, 5–0.05 μm) on a Buehler polishing cloth. In the RRDE measurements, the radius of the disk electrode was 2.3 mm, and the inner and outer radii of the ring electrode were 2.46 and 2.7 mm, respectively. The collection efficiency of the RRDE assembly was determined from the ratio of ring and disk currents (at various rotation rates) using the argon-saturated 0.005 mol dm^{-3} $K_3[Fe(CN)_6]$+0.01 mol dm^{-3} K_2SO_4 solution [7–9]. Based on five independent experiments, it was found that, within the potential range considered here, and at rotation rates up to 2,500 rpm, the experimental collection efficiency (N) remained unchanged and was equal to 0.23. During the RRDE measurements in oxygen-saturated solutions, the potential of the ring electrode was kept at 1.2 V. At this potential, the generated H_2O_2 is oxidized under diffusional control. All RDE and RRDE polarization curves were recorded at a scan rate of 10 mV s^{-1}.

Carbon (Vulcan) supported $RuSe_x$ ($RuSe_x$/C) clusters were fabricated at HMI, Berlin, using the procedure analogous to that described earlier [7]. Their composition was as follows: Ru, 20; Se, 1, and C 79% (by mass). The

diameters of carbon supports and $RuSe_x$ particles were approximately 20 and 2 nm, respectively. To produce an ink of bare $RuSe_x$/C nanoparticles, a known amount (5 mg) of the catalyst was dispersed in 480 μl of 0.9% Nafion solution (from Aldrich) and subjected to sonication for 10 min. The ink of WO_3-modified $RuSe_x$/C was produced in an analogous manner, but 20 μl of aqueous 0.012 mol dm^{-3} Na_2WO_4 solution was added as well. As a rule, 2.5 μl of aliquot of the appropriate ink was introduced onto the surface of a glassy carbon disk electrode (geometric area, 0.16 cm^2), and the suspension was air-dried at room temperature. As a rule, the catalytic films were activated by performing two to three full voltammetric potential cycles in the potential range from 0 to 0.9 V (at 50 mV s^{-1}) until steady-state currents were observed. The morphology of WO_3-modified $RuSe_x$/C nanoparticles was examined (Fig. 1) using Philips CM 10 transmission electron microscopy operating at 100 kV. $RuSe_x$ nanoparticles, which are represented by dark dots, have diameters ranging from 2 to 3 nm. The lighter areas should be attributed to larger (bulk) carbon (Vulcan) supports; but the grayish portions presumably reflect the less dense metal oxide (WO_3) overlayers. Although their thickness is on the level of tens of nanometers, they do not form coherent films. It is also likely that, while exposed to electrolyte, WO_3 is in hydrated form. In a separate X-ray photoelectron spectroscopic experiment (performed at Bessy2, Berlin, Germany), we have determined that the molar ratio of W to Ru is equal to 0.2.

Nanoparticles of carbon (Vulcan XC-72) supported platinum (with the relative metal loading of 20 wt%) were used as comparative catalysts for the oxygen electroreduction. According to the manufacturers' information, the size of Pt nanoparticles was on the level 2–3 nm. They were deposited on glassy carbon disks in a manner analogous to that described for $RuSe_x$/C nanoparticles.

The polymer electrolyte Nafion 115 membrane was utilized in PEMFC fuel cell. The membrane was cleaned as described earlier [29]. The assembly with two metallic plates was pressed at 125 °C under the pressure of 50 MPa for 2 min. During operation of the fuel cell, the pressure of hydrogen and oxygen was 1 bar, and the flow rate of both gases was 100 ml min^{-1}. Curves of the cell voltage and power versus current density were recorded at 80 °C.

Results and discussion

Typical cyclic voltammetric responses of (a) bare and (b) WO_3-modified $RuSe_x$/C nanoparticles, which have been deposited on glassy carbon electrode and investigated in the deaerated 0.5 mol dm^{-3} H_2SO_4 solution, are illustrated in Fig. 2a. The presence of tungsten oxide layers on $RuSe_x$/C

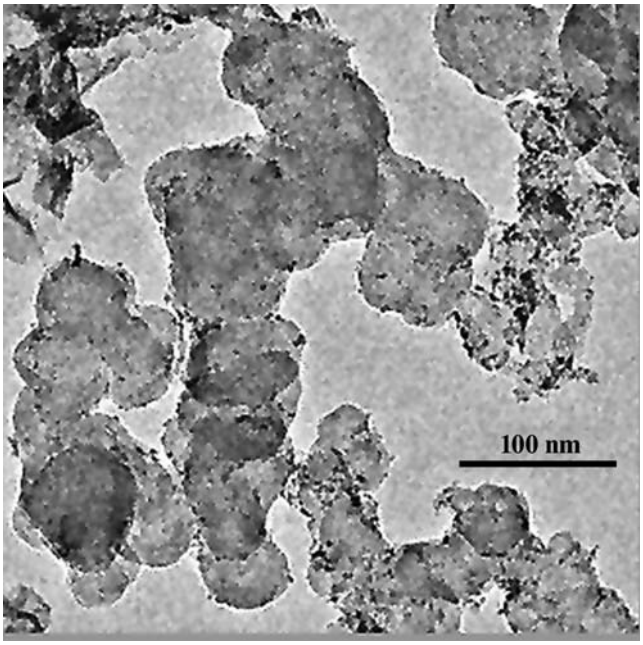

Fig. 1 Transmission electron micrograph of WO_3-modified $RuSe_x$/C nanoparticles

is evident from the existence of relatively higher voltammetric currents at potentials lower than 0.5 V (Curve b) in comparison to bare $RuSe_x$/C (Curve a). Electroactivity of WO_3 (Curve b) originates from its ability to undergo reversible reduction to nonstoichiometric oxides, such as substoichiometric hydrogen tungsten oxide bronzes (H_xWO_3, $0<x<1$) or lower tungsten oxides (WO_{3-y}, $0<y<1$) [27]. The current increases observed at potentials higher than 0.8 V in the case of both bare and WO_3-modified $RuSe_x$/C (Curves a and b in Fig. 2a) are likely to originate from the oxidation of selenium-covered metallic ruthenium. Application of potentials higher than 0.9 V for longer periods of time may lead to the degradation $RuSe_x$ catalytic centers. For comparison, we also provide the voltammetric response of Vulcan-supported Pt nanoparticles (deposited on glassy carbon) recorded in the deaerated 0.5 mol dm^{-3} H_2SO_4 (Curve c). As expected, the system is characterized at potentials below 0.3 V by the formation of hydrogen adsorption/desorption peaks, whereas oxidation of Pt to PtOH or PtO species occurs at more positive potentials.

When the Fig. 2a experiments were repeated in the oxygen-saturated 0.5 mol dm^{-3} H_2SO_4,, the characteristic oxygen reduction peaks (Fig. 2b) appeared at potentials 560 mV (Curve a) and 625 mV (Curve b) in the case of bare and WO_3-modified $RuSe_x$/C, respectively. In other words, by shifting the oxygen reduction potential towards more positive values, tungsten oxide exhibited an activation effect on $RuSe_x$/C catalytic centers. When compared to the voltammetric reduction in oxygen at Pt-catalyst (Curve c),

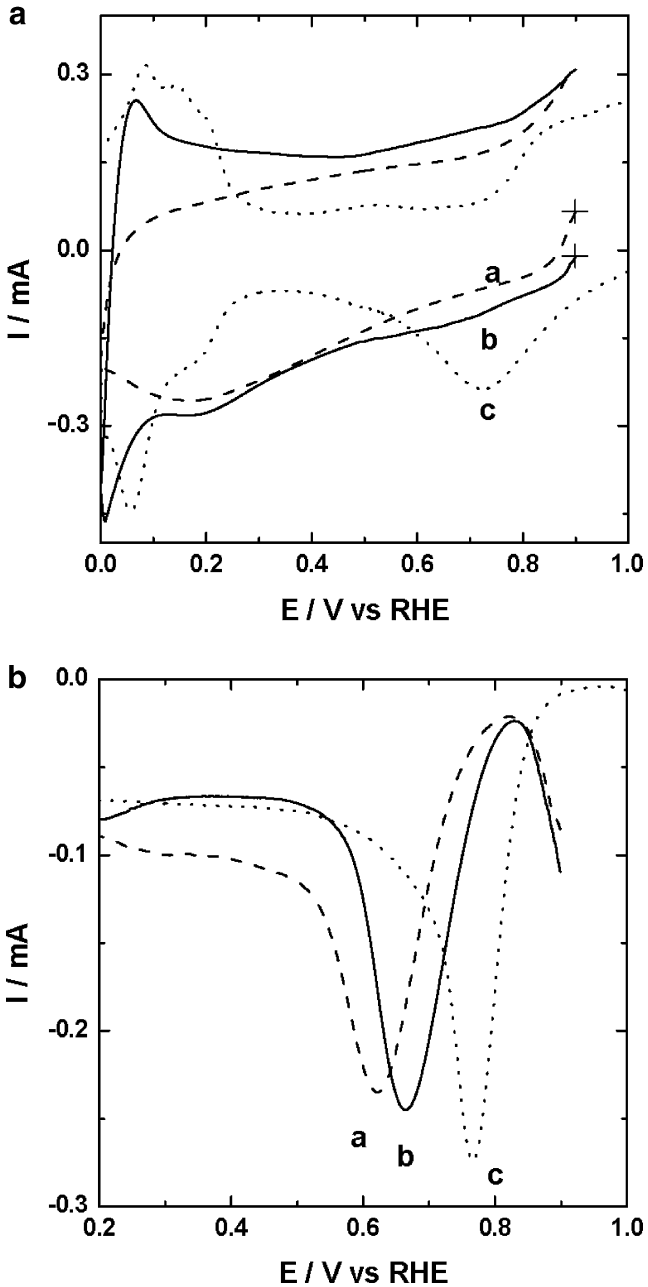

Fig. 2 **a** Background voltammetric responses of (*a*) bare and (*b*) WO_3-modified $RuSe_x/C$, and (*c*) Vulcan-supported Pt nanoparticles (deposited on glassy carbon) recorded at 50 mV s^{-1} in argon-saturated 0.5 mol dm^{-3} H_2SO_4. **b** Background-subtracted voltammograms recorded in the oxygen-saturated electrolye

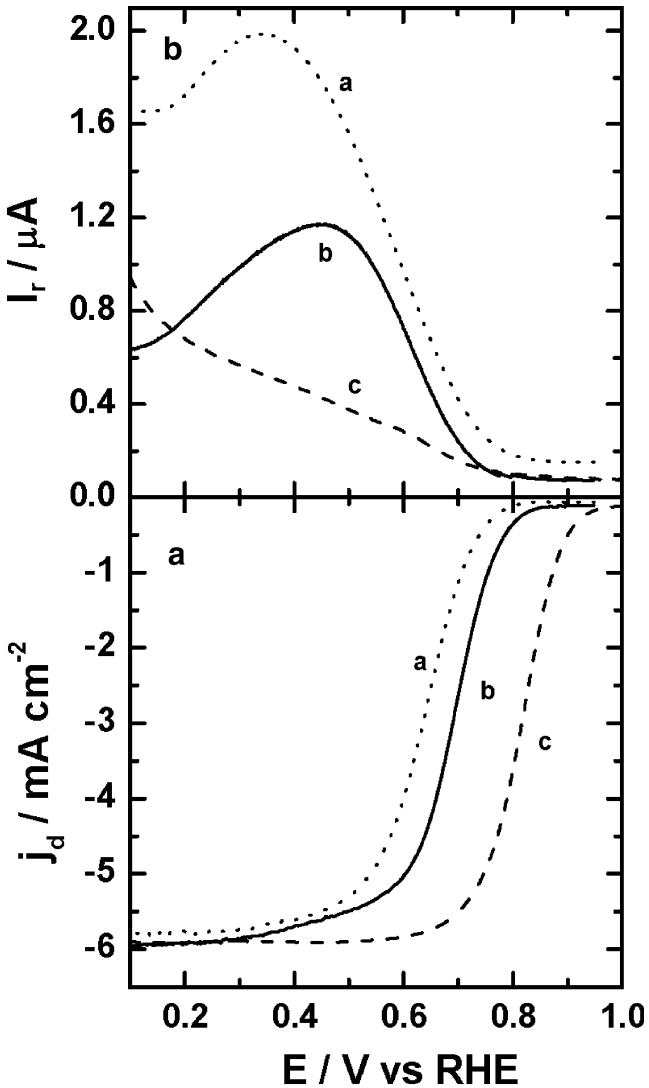

Fig. 3 RRDE voltammetric responses recorded at 10 mV s^{-1} scan rate in 0.5 mol dm^{-3} H_2SO_4 at 1,600 rpm: **a** disk currents and **b** ring currents. Curves *a*, *b*, and *c* refer to bare $RuSe_x/C$, WO_3-modified $RuSe_x/C$, and Vulcan-supported Pt nanoparticles, respectively. Ring potential, 1.2 V

the respective voltammetric peak at WO_3-modified $RuSe_x/C$ appeared at ca. 150 mV less positive potential.

To better diagnose electrocatalytic properties of the investigated systems, we have performed RDDE measurements in which inks of catalytic nanoparticles were deposited onto disk electrodes. The representative RRDE voltammograms are illustrated in Fig. 3. The responses recorded at the disk electrode (Fig. 3a) clearly show that, while electroreduction of oxygen at WO_3-modified $RuSe_x/C$ (curve b) proceeds at more positive potential (ca. 70 mV) in comparison to bare $RuSe_x/C$ (curve a), the system (even in the presence of tungsten oxide) is still catalytically less active relative to conventional Pt nanoparticles (curve c). Consequently, when recorded at Pt, the oxygen reduction currents reach limiting values at more positive potentials than in the case of $RuSe_x$-based systems. The responses recorded (upon application of the oxidative potential of 1.2 V) at the ring Pt electrode are consistent with the view that formation of hydrogen peroxide intermediate has significantly decreased after modification of $RuSe_x/C$ with tungsten oxide (compare Curves a and b in Fig. 3b). This effect is the most pronounced at potentials lower than 0.25 V where the tungsten oxide (WO_3) starts to

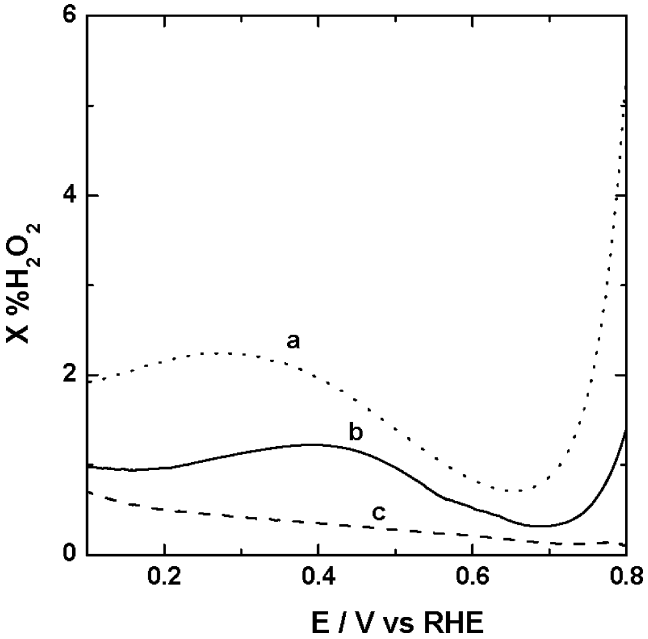

Fig. 4 Fraction of hydrogen peroxide produced during electroreduction of oxygen under the conditions of RRDE voltammetric experiment of Fig. 3

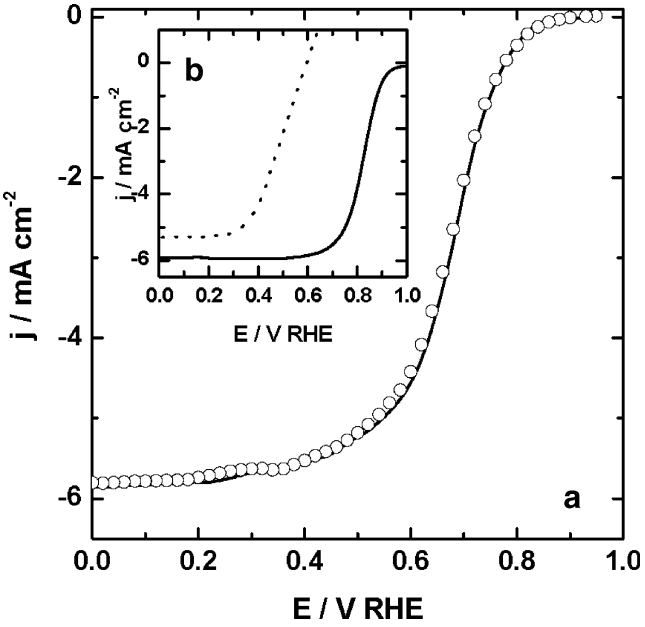

Fig. 5 Current-potential RDE curves for oxygen reduction recorded at **a** WO_3-modified $RuSe_x$/C and **b** Vulcan-supported Pt nanoparticles. *Solid lines* stand for the responses in the methanol-free oxygen saturated 0.5 mol dm^{-3} H_2SO_4. *Circles* (**a**) and the *dotted line* (**b**) refer to responses in the presence of 0.5 mol dm^{-3} methanol. Rotation rate, 1,600 rpm

be reduced to hydrogen tungsten bronzes (H_xWO_3) that are capable of inducing reduction of H_2O_2 (to H_2O). The latter observation implies direct involvement of the tungsten oxide matrix in promoting the efficient four-electron reduction in oxygen to water. Under such conditions, the bifunctional mechanism, in which both $RuSe_x$ and WO_3 are reactive namely towards oxygen and hydrogen peroxide, respectively, could be operative. However, even at potentials as high as 0.7 V, the modification of $RuSe_x$ with WO_3 leads to a relative decrease in the formation of hydrogen peroxide. Because the reactive hydrogen tungsten oxide bronzes do not exist at potentials higher than 0.25 V, the activation effect originates presumably from the strong acid properties and high availability of protons in hydrated tungsten oxides (in reality tungstic acids). It should be remembered that the effective reduction mechanism (of O_2 to H_2O) requires four protons per oxygen molecule. Alternatively, WO_3 may tend to decompose undesirable H_2O_2 through the formation of peroxy compounds and their subsequent rapid disproportionation. Nevertheless, the lowest hydrogen peroxide oxidation currents were recorded for the system utilizing Pt nanoparticles (Curve c in Fig. 3b).

More quantitative information, namely in the percent of amounts of H_2O_2 ($X_{\%H_2O_2}$), about the relative formation of hydrogen peroxide during the oxygen reduction under the RRDE voltammetric conditions has been obtained using the equation described earlier [7, 8]:

$$X_{\%H_2O_2} = 200[(I_r/N)/(I_d + (I_r/N))] \quad (4)$$

where I_r is the ring current (in A), I_d stands for the disk current (in A), and N is the dimensionless collection efficiency. The results are plotted versus potentials applied to the disk electrode in Fig. 4. At the electrode modified with inks of WO_3-modified $RuSe_x$/C nanoparticles (Curve b), the production of H_2O_2 is significantly lower in comparison to the system utilizing bare $RuSe_x$/C nanoparticles (Curve a). At potentials lower than 0.7 V, the values of $X_{\%H_2O_2}$ are fairly low, namely on the level 1% for WO_3-modified $RuSe_x$/C. At potentials higher than 0.7 V, the oxygen reduction currents (at disk electrode) are not well developed yet (Curves a and b in Fig. 4) because the potentials are not sufficiently negative to drive effectively the oxygen reduction reaction; consequently, the values of $X_{\%H_2O_2}$ has become somewhat higher. In the whole range of investigated potentials, the lowest percent formation of hydrogen peroxide has been obviously observed in the case of the Pt catalyst (Fig. 4).

It was reported that, while $RuSe_x$ was largely methanol-tolerant, the electrocatalytic activity of Pt towards the reduction in oxygen significantly decreased in the presence of methanol [24]. Our present results (Fig. 5) clearly show that the RDE voltammetric responses recorded (at 1,600 rpm) in the oxygen-saturated 0.5 mol dm^{-3} H_2SO_4 with the use of the WO_3-modified $RuSe_x$/C catalyst are almost identical in the presence (circles) and in the absence (solid line) of 0.5 mol dm^{-3} methanol. When the analogous experiments have been repeated at catalytic Pt nanoparticles

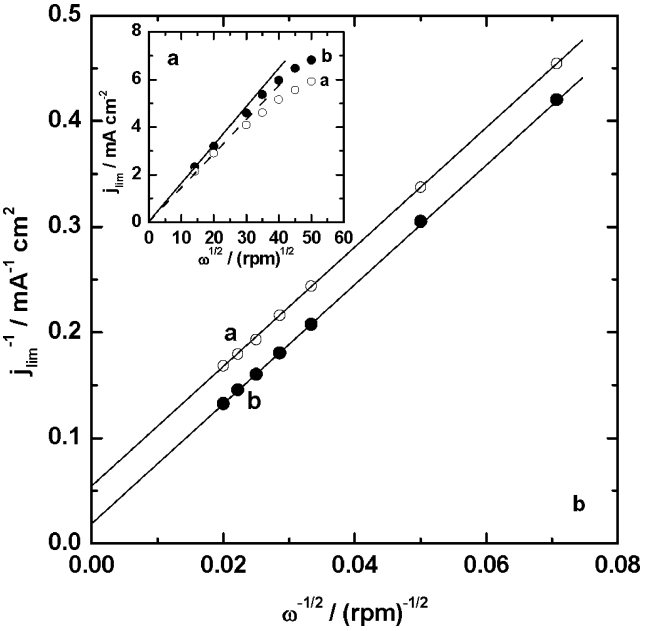

Fig. 6 **a** Levich plots and **b** Koutecky–Levich reciprocal plots (prepared using the data of Fig. 3) for the electroreduction of oxygen (at 0.5 V) at catalytic layers (deposited on glassy carbon disks) containing (*a*) bare and (*b*) WO_3-modified $RuSe_x$/C nanoparticles. Loadings of $RuSe_x$, 150 μg cm^{-2}

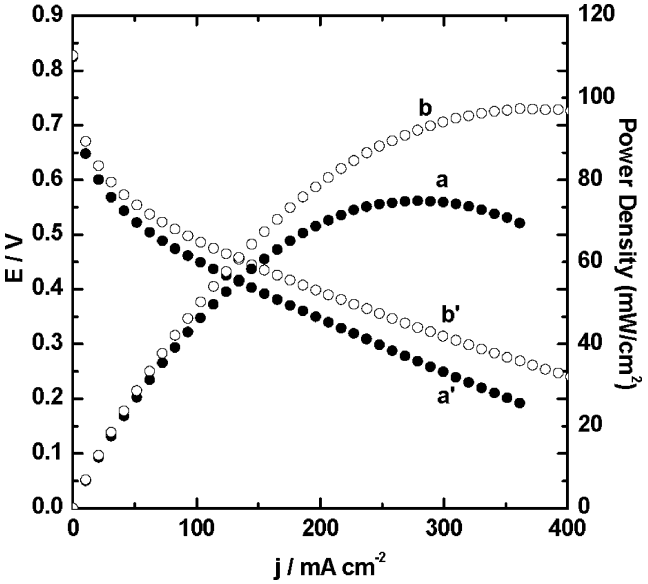

Fig. 7 Dependencies of fuel cell (PEMFC) power densities and voltage on current density for bare (*a* and *a′*) as well as WO_3-modified $RuSe_x$/C (*b* and *b′*) catalytic nanoparticles. Loadings of the platinum anode catalyst and the $RuSe_x$ cathode catalysts, 0.4 mg cm^{-2}

(Inset to Fig. 5), the oxygen reduction has started to occur in the methanol-containing solution at about 0.6 V (dotted line), i.e., approximately 300 mV more negative in comparison to the behavior at Pt in the absence of methanol (solid line). Apparently, simultaneous oxygen reduction and oxidation of methanol that can take place on platinum have led to the drop in the system's cathodic potential. Contrary to Pt, WO_3-modified $RuSe_x$/C can be viewed as the methanol-tolerant oxygen reduction catalyst. Apparently, unlike Pt, methanol is unable to chemisorb on $RuSe_x$ even in the presence of activating WO_3.

We subjected the results of RDE voltammetric experiments, in which (a) WO_3-free and (b) WO_3-modified $RuSe_x$/C electrocatalysts were utilized, to kinetic analysis. When RDE oxygen reduction current densities measured at 0.5 V were plotted versus the square root of the rotation rates (Levich plots; Fig. 6a), the deviation from linearity (i.e., from the ideal behavior characteristic of systems limited solely by convective diffusion of oxygen in the solution) was more pronounced at bare rather than the WO_3-modified system. Apparently, the catalytic activity of WO_3-free $RuSe_x$/C was less effective in comparison to WO_3-modified $RuSe_x$/C nanoparticles. We have further analyzed the results by means of the so-called Koutecky–Levich reciprocal plots (Fig. 6b) [25, 27]. In this study, the assumption was made that only such factors as transport of oxygen in solution or at higher rotation rates the dynamics of the catalytic reaction were rate-determining steps. The fact that reciprocal plots (Curves a and b in Fig. 6b) yielded nonzero intercepts indicated kinetic limitations associated with the electrocatalytic film. To estimate heterogeneous rate constants from the data of Fig. 6b, the following dependence of the reciprocal of limiting current (I_{lim}) was considered:

$$\frac{1}{I_{\text{lim}}} = \frac{1}{nFAkC_{\text{film}}C_{O_2}} + \frac{1}{I_d} \tag{5}$$

where I_d was the ideal convective-diffusional current described according to the Levich equation, k was the homogeneous rate constant of the catalytic reaction, F stood for the Faraday constant, C_{film} was the surface concentration of the catalytic sites, C_{O_2} was the bulk (solution) concentration of oxygen (ca. 1.1 mmol dm^{-3} in 0.5 H_2SO_4 [28]), and n was the number of electrons transferred. The values of kC_{film}, which were equivalent to the intrinsic rates of heterogeneous charge transfer, were 9.5×10^{-2} and 3×10^{-2} cm s^{-1} for the oxygen electroreduction (at 0.5 V) at the glassy carbon disk covered with WO_3-modified $RuSe_x$/C and bare $RuSe_x$/C nanoparticles. The above results were reproducible within 5–10% in different experiments. Thus, modification of $RuSe_x$/C with ultra-thin layers of WO_3 resulted in more than three time increases in the heterogeneous rate constant for oxygen reduction. Finally, no dissolution of WO_3 (from the catalysts deposited as inks

on glassy carbon using Nafion ionomer) has been observed during voltammetric (including RRDE) experiments.

The $RuSe_x$-based electrocatalytic materials were also tested in hydrogen–oxygen fuel cell (PEMFC) in which anode was formed from Pt nanoparticles (capable of catalyzing hydrogen oxidation) and the cathode utilized (a) bare and (b) WO_3-modified $RuSe_x$/C nanoparticles. Before sandwiching the Nafion membrane between two pieces of carbon paper, the catalysts were first distributed onto its surface. The fuel cell was tested by recording dependencies of the cell voltage and power density against the current density at 80 °C (Fig. 7). The maximum power densities were ca. 75 and almost 100 mW cm^{-2} for cathodes composed of (a) bare and (b) WO_3-modified $RuSe_x$/C catalysts, respectively. While the initial open circuit voltages were comparable on the level 0.85 V, larger cell voltages were obtained at the same current densities (shown up to 400 mA cm^{-2} in Fig. 7) in the case WO_3-modified $RuSe_x$/C.

Conclusions

On the basis of our RRDE diagnostic experiments and preliminary results with the PEMFC fuel cell, it can be concluded that the modification of $RuSe_x$/C nanoparticles with tungsten oxide results in their activation towards oxygen reduction. The phenomenon can originate from the acidic properties of WO_3, and at potentials lower than 0.25 V, it reflects the formation of hydrogen tungsten oxide bronzes and the system's ability to catalyze the reduction in the hydrogen peroxide intermediate. Specific interactions between WO_3 and $RuSe_x$, although not documented as yet, cannot be excluded. Further research is along this line. Mutual activating interactions between tungsten oxide matrix and Pt catalytic centers were historically found or postulated [27, 30, 31]. Finally, the WO_3-modified $RuSe_x$/C is practically completely methanol tolerant. This observation could be of particular importance to the application in the mixed-reactants solid-polymer-electrolyte direct methanol fuel cells [32] in which mixtures of methanol with oxygen (or air) were successfully supplied to the anode compartment. Under such conditions, higher liquid saturation in the anode diffusion layer of DMFC and faster removal of the carbon dioxide product were postulated [33].

Acknowledgment The Warsaw group appreciates the support from the Ministry of Science and National Education (Poland) (N204 164 32/4284). This work has also been supported by the Network of Efficient Oxygen Reduction for Electrochemical Energy Conversion (coordinated by ZSW, Ulm, Germany). Partial support by the Ministero dell'Istruzione dell'Università e della Ricerca (MIUR), Italy, under the project FISR 2001 is also acknowledged.

References

1. Perry ML, Fuller TF (2002) J Electrochem Soc 149:S59
2. Xia C, Lang Y, Meng G (2004) Fuel Cell 4:41
3. Helmolt R (2004) Fuel Cell 4:264
4. Cropper M (2004) Fuel Cell 4:236
5. Shukla AK, Raman RK (2003) Annu Rev Mater Res 33:155
6. Albery WJ, Hitchman ML (1971) Ring-disc electrodes. Clarendon, Oxford
7. Bron M, Bogdanov P, Fiechter S, Dorbandt I, Hilgendorff M, Schleburg H, Tributsch H (2001) J Electroanal Chem 500:510
8. Stamenkovic V, Schmidt TJ, Ross PN, Markovic NM (2003) J Electroanal Chem 554–555:191
9. Bard AJ, Faulkner LR (2001) Electrochemical methods: fundamentals and applications. Wiley, New York
10. Galus Z (1994) Fundamentals of electrochemical analysis (2nd edn). Wiley, New York
11. Markovic NM, Schmidt TJ, Stamenkovic V, Ross PN (2001) Fuel Cell 1:105
12. Zhang J, Lima FHB, Shao MH, Sasaki K, Wang JX, Hanson J, Adzic RR, (2005) J Phys Chem B 109:22701
13. Ioroi T, Yasuda K (2005) J Electrochem Soc 152:A1917
14. Yang H, Alonso-Vante N, Lamy C, Akins DL (2005) J Electrochem Soc 152:A704
15. Gupta S, Tryk D, Zecevic SK, Aldred W, Guo D, Savinell RF (1998) J Appl Electrochem 28:673
16. Gojkovic SLJ, Gupta S, Savinell RF (1999) J Electroanal Chem 462:63
17. Kalvelage H, Mecklenburg A, Kunz U, Hoffmann U (2000) Chem Eng Technol 23:803
18. Dokiya M (2002) Solid State Ionics 152–153:383
19. Molenda J, Nowak I, Jedynak L, Marzec J, Stoklosa A (2000) Solid State Ionics 135:235
20. Yamamoto O (2000) Electrochim Acta 45:2423
21. Alonso-Vante N, Bogdanoff P, Tributsch H (2000) J Catal 190:240
22. Sebastian PJ, Rodriguez FJ, Solorza O, Rivera R (1999) J New Mater Electrochem Syst 2:115
23. Tributsch H, Bron M, Hilgendorff M, Schulenburg H, Dorbandt I, Eyert V, Bogdanoff P, Fiechter S (2001) J Appl Electrochem 31:739
24. Cao D, Wieckowski A, Inukai J, Alonso-Vante N (2006) J Electrochem Soc 153:A874
25. Kulesza PJ, Miecznikowski K, Baranowska B, Skutnik M, Fiechter S, Bogdanoff P, Dorbandt I (2006) Electrochem Commun 8:904
26. Zaikovskii VI, Nagabhushana KS, Kriventsov VV, Loponov KN, Cherepanova SV, Kvon H, Bonnemann RI, Kochubey DI, Savinova ER (2006) J Phys Chem B 110:6881
27. Kulesza PJ., Grzybowska B, Malik MA, Galkowski MT (1997) J Electrochem Soc 144:1911
28. Zecevic SK, Wainright JS, Litt MH, Gojkovic S Lj, Savinell RF (1997) J Electrochem Soc 144:2973
29. Paganin VA, Ticianelli EA, Gonzalez ER (1996) J Appl Electrochem 26:297
30. Kulesza PJ, Faulkner LR (1989) J Electroanal Chem 259:81
31. Colemenares L, Jusys Z, Kinge S, Bonnemann H, Behm RJ (2007) J New Mater Electrochem Syst (in press)
32. Scott K, Shukla AK, Jackson CL, Meuleman WRA (2004) J Power Sources 126:67
33. Shukla AK, Jackson CL, Scott K, Murgia G (2002) J Power Sources 111:43